High-power 120 fs pulses at 1.23 GHz from a single-mode Er-Yb-doped Fiber laser

MELIH KAYRA KADIOGLU,[1] BURAK ASLAN,[2] AND PARVIZ ELAHI[3,*]

[1] *Department of Physics, Koç University, 34450 Istanbul, Türkiye*
[2] *Department of Physics, Boğaziçi University, 34342 Istanbul, Türkiye*
[3] *Department of Natural and Mathematical Sciences, Özyeğin University, 34794 Istanbul, Türkiye*
[*] *parviz.elahi@ozyegin.edu.tr*

Abstract: We present a compact single-mode Erbium-doped master oscillator power amplifier (MOPA) fiber laser that can directly produce 100 fs pulses at 2.2 W and 120 fs pulses at 4.5 W average power. The laser operates at a 1.2 GHz pulse repetition rate, with a central wavelength around 1550 nm. The laser system consists of a passively mode-locked oscillator with a repetition rate of 77.6 MHz and an average power of 16.3 mW. Using a repetition rate multiplier consisting of six 50/50 couplers, we achieved pulses with a repetition rate of 1.23 GHz. The output was subsequently increased to approximately 4.5 W average and 30 kW peak power using a cladding pump 10/125 Erbium-Ytterbium (Er-Yb) doped gain fiber. Through numerical modeling of pulse generation within the laser, we achieved a very good agreement with experimental results, inferring the pulse dynamics and its power scaling limitations.

1. Introduction

The generation of ultrafast laser pulses, particularly in the femtosecond regime, has been a subject of significant research due to its numerous applications in fields such as ultrafast spectroscopy [1–3], optical communication [4, 5], and material processing [6–8]. Among various laser sources, erbium-doped fiber lasers (EDFLs) have garnered considerable attention due to their ability to operate in the 1.55 µm region, which is essential for telecommunication applications [9] and subsurface laser processing of materials such as silicon [10, 11]. Ultrafast lasers with GHz pulse repetition rates hold significant potential across various fields. In frequency metrology [12, 13], they enable precise time and frequency measurements. Their ability to generate arbitrary waveforms makes them invaluable in advanced signal processing and optical telecommunications, where they can significantly enhance data transmission speeds and bandwidth. In biomedicine [14, 15], these lasers facilitate high-resolution imaging and minimally invasive surgical procedures. In laser material processing [16, 17], ultrafast fiber lasers with GHz-range pulse repetition rate provide high precision and efficiency in cutting, drilling, and surface modification.

We introduced a new regime of ultrafast laser material processing, which we call ablation-cooled material removal [18]. In this regime, cooling of the material co-occurs with ablation, as the pulses are repeated at intervals short enough to limit heat diffusion from the targeted area to the surroundings. With each successive pulse, the targeted material heats up to the critical temperature needed for evaporative removal. The ablation process then removes a substantial portion of the thermal energy localized at the targeted spot, consequently significantly increasing the ablation efficiency. This regime is reached by delivering pulses at a GHz repetition rate. Thus, the development of fiber lasers capable of generating such high repetition rates has drawn significant attention.

H. Byun et al. [19] reported 187 fs pulses at a repetition rate of 967 MHz using a soliton fiber laser based on highly doped anomalously dispersive erbium-doped fiber. A stable passively mode-locked Er fiber laser with a fundamental repetition rate of up to 5 GHz was presented by X. Gao et al. [20]. All-fiber passively mode-locked lasers producing subpicosecond pulses with 19.45 GHz fundamental repetition rates were reported in [21]. Very recently, Z. Chen et al. [22]

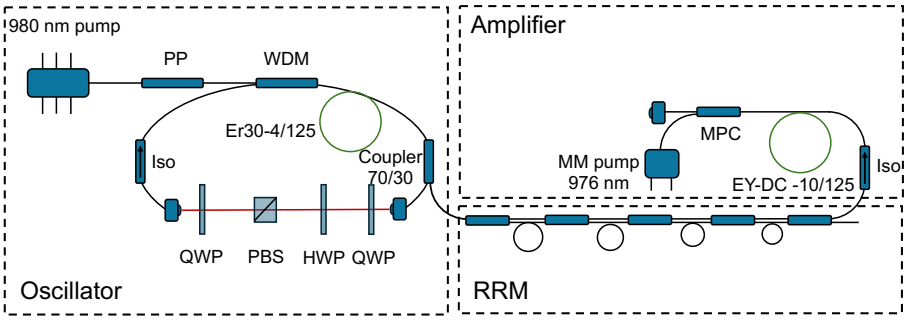


Fig. 1. Schematic of the laser setup: PP: pump laser protector, QWP: quarter wave plate, HWP: half-wave plate, PBS: polarizing beam splitter, RRM: repetition rate multiplier, MM pump: multi-mode pump, MPC: multi-mode pump signal combiner, Iso: isolator, WDM: Wavelength-division multiplexing

demonstrated 1 GHz femtosecond erbium-doped fiber ring laser mode-locked, which delivers a maximum average output power of 228 mW. In the mentioned works, the high repetition rate pulses generated from the oscillator such that their average power/peak power is too low for laser material processing. There are several reports on the development of high-power fiber lasers with GHz-range pulse repetition rates using large mode area (LMA) fibers [23–25].

In 2021, X. Chen and colleagues [26] demonstrated a high-power femtosecond all-fiber laser system operating at 1.5 µm with a fundamental repetition rate of up to 4.9 GHz, using fibers with a 10 µm core diameter. The system produced 63 fs pulses with an average power of 10.9 W, corresponding to approximately 2.2 nJ pulse energy and about 35 kW peak power. Four amplifier stages were utilized to achieve the desired output power.

Here, we present an all-fiber high-power ultrafast laser constructed from single-mode fiber, operating at a central wavelength of approximately 1550 nm and generating pulses at a 1.23 GHz repetition rate. Utilizing a single-stage amplifier and soliton pulse compression, we achieved 120 fs pulses with an average power of 4.5 W, corresponding to 3.6 nJ pulse energy and 30.5 kW peak power.

2. Experimental setup and measurements

The schematic configuration illustrated in Fig. 1 comprises a passively mode-locked oscillator, a repetition rate multiplier (RRM), and one amplifier stage. A mode-locked erbium fiber oscillator served as the seed source, operating in the anomalous dispersion regime, utilizing nonlinear polarization evolution (NPE) as the saturable absorption mechanism. The optical fiber segment within the oscillator cavity consists of a total of 1.2 m-long SMF28 with anomalous dispersion ($\beta_2 = -22.8\,\mathrm{fs}^2/\mathrm{mm}$ at 1550 nm), and 1.3 mm-long Er-doped fiber (Er30-4/125) with a normal dispersion ($\beta_2 = 33\mathrm{fs}^2/\mathrm{mm}$ at 1550 nm, 30 dB/mm peak absorption at 1530). The net cavity dispersion is estimated to be approximately $15540\,\mathrm{fs}^2$ at the central wavelength of 1550 nm. A single-mode fiber-pigtailed laser diode pumps the oscillator at 980 nm. Self-started mode-locking is achieved with 410 mW pump power. It produces an average power of 21 mW through the 30% port of the output coupler inserted after the gain fiber. The central wavelength is about 1560 nm, and the pulse repetition rate is measured as 77.6 MHz. The mode-lock operation is self-started and stable. To achieve sufficient power and broaden the spectral width, we increased the pump power to 880 mW, resulting in a 45 mW signal power. The intensity autocorrelation trace (measured by FR-103XL, Femtochrome Research Inc.) of the output pulse of the oscillator from the same output coupler is shown in Fig. 2a. The measured pulse width is about 1.48 ps, assuming a sech pulse shape profile. At 45 mW output power, the optical spectrum, displayed in

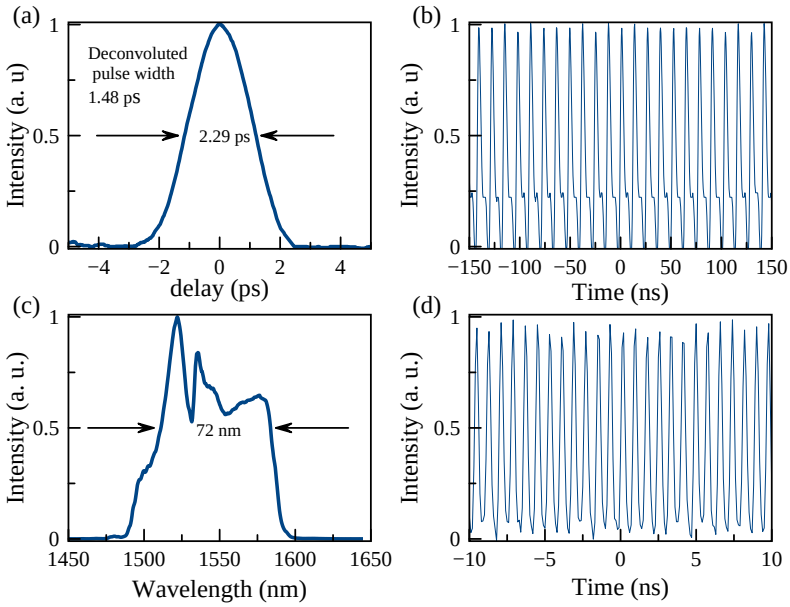


Fig. 2. Experimental results: The measured (a) intensity autocorrelator, (b) pulse train, and (c) optical spectrum of the mode-locked oscillator from 30% port of the output coupler at 45 mW average power. (d) 1.23 GHz pulse train after the repetition rate multiplier

Fig. 2c, has a full width at half maximum (FWHM) of approximately 72 nm.

To increase the pulse repetition rate from MHz to GHz, the output from the oscillator is directed towards the repetition rate multiplier, as illustrated in Fig. 1. This multiplier comprises a series of cascaded 3-dB couplers, where each coupler features a length difference between its two output arms. This difference equates to a delay equivalent to half the signal repetition rate period at the input of that specific coupler. Consequently, the repetition rate is doubled at each stage. With five successive couplers, the repetition rate experiences a sixteen-fold increase, increasing from 77.6 MHz to 1.24 GHz (Fig. 2d).

Following the repetition rate multiplier, the output power of 16.3 mW, after passing through a high power isolator, is amplified to 5 W (4.5 W after collimator) through a backward pumping single amplifier stage. This stage incorporates a 1.3-m-long double-clad co-doped EY gain fiber (DCF-EY, 10/128, CorActive, Inc.). The cladding absorption coefficient of the gain fiber at 915 nm is 2.4 dB/m. A multi-mode pump-signal combiner (MPC) is employed to deliver pump light from a wavelength-stabilized diode laser (BWT, Inc.) at 980 nm to the cladding region of the gain fiber. The maximum output power of the pump diode is 18 W, which allows us to scale up the average output power of the amplifier to 4.5 W at a pump power of 12 W. To collimate the output laser beam, we spliced a single-mode high-power collimator to the signal port of the MPC. The power is maintained at this level to prevent damage to the subsequent collimator.

The laser output is directed to a characterization setup comprising an optical spectrum analyzer, autocorrelator, and power meter for simultaneous measurement. The measured intensity autocorrelation at different outpower powers, 1.5 W, 2 W, 2.2 W, 3 W, 4 W, and 4.5 W, is shown in Fig. 3a. The full-width at half-maximum (FWHM) pulse duration by considering Sech2-shaped pulse is estimated to be 774 fs, 285 fs, 100 fs, 183 fs, 163 fs, and 122 fs, respectively. This figure shows that the shortest pulse duration is 100 fs at 2.2 W output power, corresponding to about 1.8 nJ pulse energy and 18 kW peak power.

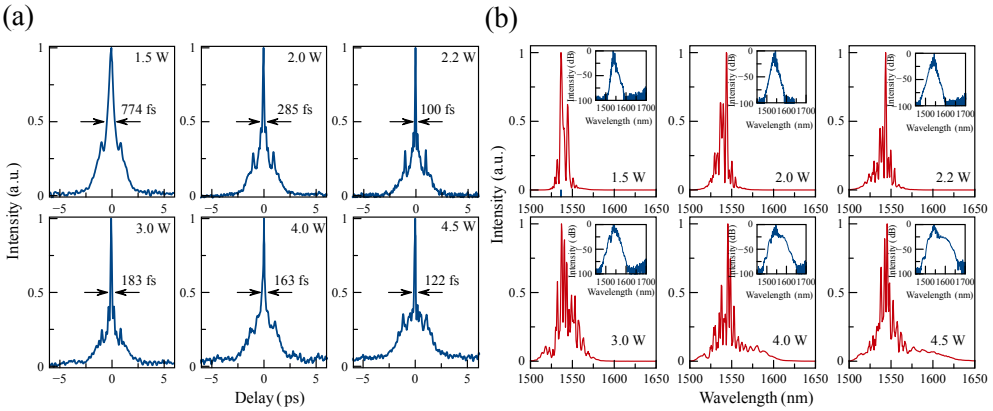


Fig. 3. Experimental results: (a) intensity autocorrelations and (b) optical spectra at different output powers. The inset shows the optical spectra in semi-log.

Figure 3b shows the optical spectra measured at different output powers. Due to the gain narrowing mechanism, the spectral width reaches approximately 10 nm at 1.5 W output power, but it begins to increase due to nonlinearity. Nearly all of the nonlinear pulse shaping in the system occurs within the last 3.2 m passive fiber (SMF-28) after the gain segment. At average powers of 2.2 W and 4.5 W, the initial peak power is about 18 kW and 30 kW, respectively. The corresponding estimated nonlinear phase shift accumulated in the passive fiber is approximately 19.5π and 32.5π, respectively. As pulse energy increases, nonlinear effects intensify, causing rapid spectral broadening. Raman scattering generates at average power of about 4 W, but still, at 4.5 W, it is insignificant. Raman and self-phase modulation (SPM) results in asymmetrical spectral broadening, which generates a linear frequency chirp and cannot be compensated during pulse compression. The residual energy in the pulse wings appears as the pedestal (Fig. 3a) [26].

3. Numerical simulations

Numerical simulations are utilized to investigate the pulse dynamics across the entire system. The oscillator's output provides the initial condition for this propagation, which serves as the initial condition for the subsequent stages involving the repetition rate multiplier and the amplifier. The pulse propagation within each medium is simulated using the generalized nonlinear Schrödinger equation, which incorporates the third-order dispersion (TOD), gain with saturation, and Raman scattering.

$$\frac{\partial A}{\partial z} + i\frac{\beta_2}{2}\frac{\partial^2 A}{\partial \tau^2} - \frac{\beta_3}{6}\frac{\partial^3 A}{\partial \tau^3} - \frac{g}{2}A - i\gamma|A|^2 A - i\gamma T_R \frac{\partial |A|^2}{\partial \tau} - \delta\frac{\partial^2 A}{\partial \tau^2}A = 0 \quad (1)$$

where $A(z,t)$ is the slowly varying complex pulse envelope, z is the propagation coordinate, τ is the retarded time, β_2 is the group velocity dispersion coefficient, β_3 is the third-order dispersion coefficient, $\gamma = n_2\omega_0/cA_{eff}$ is the effective nonlinear coefficient, where n_2 is the nonlinear refractive index, ω_0 is the angular frequency at the central frequency, and A_{eff} is the effective beam area, δ_p represents the gain saturation effect, and T_R is related to the slope of the Raman gain spectrum and $g = \frac{g_s}{1+\frac{\int |A|^2 d\tau}{E_{sat}}}$ represents the net gain, where, g_s represents the small signal gain E_{sat} stands for saturation energy. The governing equation is solved by the standard split-step

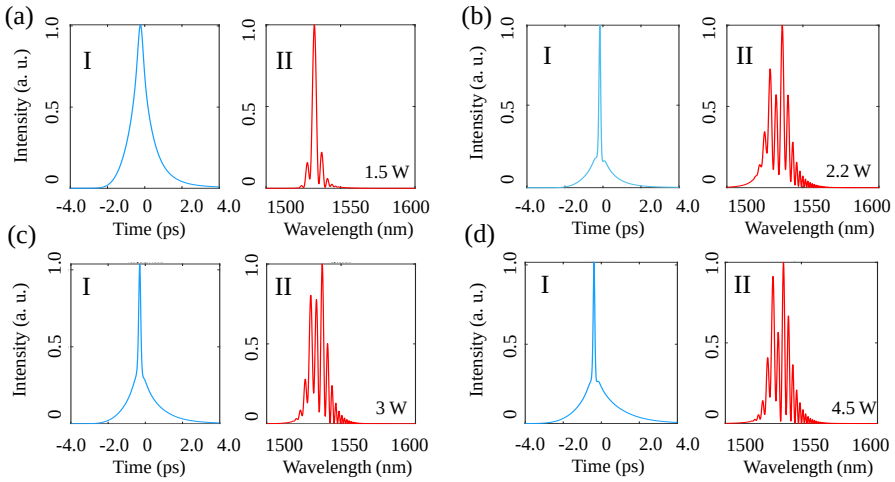


Fig. 4. Numerical simulation results: The output pulse shape (I) and corresponding optical spectrum (II) at different average powers, (a) 1.5 W, (b) 2.2 W, (c) 3 W, and (d) 4.5 W.

method. The following are the parameters used for the fiber segments: $\beta_2 = -23\,\mathrm{fs}^2/\mathrm{mm}$ (at 1550 nm), $n_2 = 2.3 \times 10^{-16}\,\mathrm{cm}^2/\mathrm{W}$, the gain bandwidth is 33.3 nm, $\gamma = 1.1\ 1/\mathrm{W}\cdot\mathrm{km}$, $E_{\mathrm{sat}} = 1.8\,\mathrm{nJ}$, and $g_s = 44.5\,\mathrm{dB}$.

Figure 4 depicts the simulation of the output pulse shape and the corresponding optical spectra.

Figure 5a displays the simulated results for pulse duration (blue) and spectral width (red) as a function of position within the fiber. As the pulse propagates through the coupler (following the oscillator) and the RRM, the spectral width stays approximately constant at 55 nm while the pulse duration increases from 1.5 ps to 10 ps. Considering the 75 cm length of the coupler and 8.1 m long RRM, the chirp of the pulse output from the collimator and RRM are estimated to be -1560 fs^2 and -186240 fs^2, respectively. The soliton order, N, can be calculated as

$$N^2 = \frac{\gamma \bar{E} \tau_{\mathrm{FWHM}}}{3.525\,|\beta_2|}, \tag{2}$$

Considering an average output power of 16.3 mW from the RRM, which corresponds to a pulse energy of 13.25 pJ and a maximum pulse duration of 10 ps, the maximum value of N before the gain fiber is calculated to be 0.4. In the gain fiber, based on the average pulse energy as $\bar{E} = \frac{P_0}{f_r}\frac{\exp(gL)-1}{gL}$, where P_0=13.8 mW is the seed power (by considering 15% insertion loss of the isolator), and $\exp(gL)$=5000/13.8=362 (5W power after the gain fiber), and L=1.3 m length of the gain fiber, the soliton order, N is calculated as $\sim$ 3.1 and the pulse compression factor [26] of $\sim$ 12.7 is obtained, which gives $\sim$ 867 fs pulse duration after the gain fiber. This value is approximately half of the results obtained from the simulation. As shown in Fig. 5a, self-phase modulation (SFM) causes spectrum compression in the gain fiber due to the negative initial chirp of the pulse, which also impacts the pulse evolution mechanism. The spectrum and pulse duration continue to decrease in the passive fiber following the gain fiber but at a slower slope. The spectral width decreases to a minimum of approximately 2.5 nm, then increases, reaching around 13 nm at the output. Figure 5b shows the output pulse duration versus output power simulation and the experimental results.

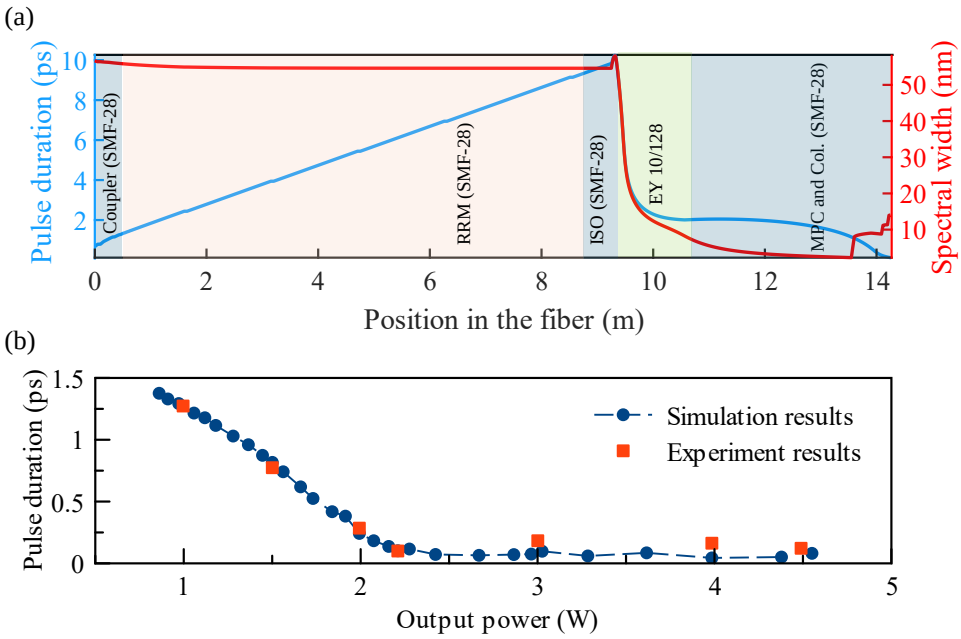


Fig. 5. Numerical simulation and experiment results : (a) The numeric simulation of variation of the spectral (red) and temporal (blue) width (FWHM) along the length of the laser starting from the output of the oscillator at 4.5 W output power. (b) The pulse duration at different output powers from the simulation (blue circles) and experiment (red squares).

4. Conclusion

We have demonstrated a compact ultrafast Er fiber laser-amplifier system capable of producing 4.5 W of average output power, corresponding to 3.65-nJ pulse energy at a 1.23-GHz repetition rate. Using a single stage of the amplifier comprising single-mode fibers, we directly obtained 120 fs pulses corresponding to ~ 30.5 kW peak power. Numerical pulse propagation in the laser system guided and verified the experimental setup. There are two opposing effects: the Raman effect, which increases with the length of the passive fiber after the gain fiber and shifts the pulses towards longer wavelengths, and nonlinear pulse compression, which requires a longer fiber. We optimized the length of the passive fiber to achieve the minimum pulse duration at the output while keeping the Raman effect insignificant.

To the best of our knowledge, this system produces the highest peak power in the multi-watt power at GHz repetition rate range for single-mode Er-doped lasers by using only one amplifier stage. The developed system has potential applications in 3D silicon processing or 3D printing through two-photon polymerization following a second-harmonic generation using GHz pulses.

Acknowledgment

This work is supported by the Higher Education Council of Türkiye (YÖK) under project number 19744 and by TÜBİTAK (Project no: 118C325).

References

1. W. Demtröder, *Laser spectroscopy 1: basic principles* (Springer, 2014).
2. M. R. Leahy-Hoppa, J. Miragliotta, R. Osiander, *et al.*, "Ultrafast laser-based spectroscopy and sensing: applications in libs, cars, and thz spectroscopy," Sensors **10**, 4342–4372 (2010).

3. G. D. Reid and K. Wynne, "Ultrafast laser technology and spectroscopy," Encycl. Anal. chemistry **35**, 13644–13670 (2000).
4. O. Wada, "Femtosecond all-optical devices for ultrafast communication and signal processing," New J. Phys. **6**, 183 (2004).
5. Y. Zhao, P. Guo, X. Li, and Z. Jin, "Ultrafast photonics application of graphdiyne in the optical communication region," Carbon **149**, 336–341 (2019).
6. K. Sugioka and Y. Cheng, "Ultrafast lasers—reliable tools for advanced materials processing," Light. Sci. & Appl. **3**, e149–e149 (2014).
7. M. Malinauskas, A. Žukauskas, S. Hasegawa, *et al.*, "Ultrafast laser processing of materials: from science to industry," Light. Sci. & Appl. **5**, e16133–e16133 (2016).
8. J. R. V. de Aldana, P. Moreno, and L. Roso, "Ultrafast lasers: A new frontier for optical materials processing," Opt. Mater. **34**, 572–578 (2012).
9. D. Brida, G. Krauss, A. Sell, and A. Leitenstorfer, "Ultrabroadband er: fiber lasers," Laser & Photonics Rev. **8**, 409–428 (2014).
10. I. Pavlov, O. Tokel, S. Pavlova, *et al.*, "Femtosecond laser written waveguides deep inside silicon," Opt. Lett. **42**, 3028–3031 (2017).
11. O. Tokel, A. Turnalı, G. Makey, *et al.*, "In-chip microstructures and photonic devices fabricated by nonlinear laser lithography deep inside silicon," Nat. photonics **11**, 639–645 (2017).
12. A. Bartels, D. Heinecke, and S. A. Diddams, "10-ghz self-referenced optical frequency comb," Science **326**, 681–681 (2009).
13. O. Kliebisch, D. C. Heinecke, S. Barbieri, *et al.*, "Unambiguous real-time terahertz frequency metrology using dual 10 ghz femtosecond frequency combs," Optica **5**, 1431–1437 (2018).
14. H. Studier, H. G. Breunig, and K. König, "Comparison of broadband and ultrabroadband pulses at mhz and ghz pulse-repetition rates for nonlinear femtosecond-laser scanning microscopy," J. Biophotonics **4**, 84–91 (2011).
15. A. Ehlers, I. Riemann, S. Martin, *et al.*, "High (1ghz) repetition rate compact femtosecond laser: A powerful multiphoton tool for nanomedicine and nanobiotechnology," J. applied physics **102** (2007).
16. H. Kalaycıoğlu, P. Elahi, Ö. Akçaalan, and F. Ö. Ilday, "High-repetition-rate ultrafast fiber lasers for material processing," IEEE J. selected topics quantum electronics **24**, 1–12 (2017).
17. X. Wolters, G. Bonamis, K. Mishchick, *et al.*, "High power ghz femtosecond laser for ablation efficiency increase," Procedia Manuf. **36**, 200–207 (2019).
18. C. Kerse, H. Kalaycıoğlu, P. Elahi, *et al.*, "Ablation-cooled material removal with ultrafast bursts of pulses," Nature **537**, 84–88 (2016).
19. H. Byun, M. Y. Sander, A. Motamedi, *et al.*, "Compact, stable 1 ghz femtosecond er-doped fiber lasers," Appl. Opt. **49**, 5577–5582 (2010).
20. X. Gao, Z. Zhao, Z. Cong, *et al.*, "Stable 5-ghz fundamental repetition rate passively sesam mode-locked er-doped silica fiber lasers," Opt. Express **29**, 9021–9029 (2021).
21. A. Martinez and S. Yamashita, "Multi-gigahertz repetition rate passively modelocked fiber lasers using carbon nanotubes," Opt. express **19**, 6155–6163 (2011).
22. C. Zhendong, R. Yang, Y. Tang, *et al.*, "Ghz fundamental repetition rate femtosecond er: fiber laser mode locked by nonlinear polarization evolution," preprints.opticaopen (2024).
23. Y. Fan, H. Xiu, W. Lin, *et al.*, "Nonlinear chirped pulse amplification for a 100-w-class ghz femtosecond all-fiber laser system at 1.5 m," High Power Laser Sci. Eng. **11**, e50 (2023).
24. J. Nicholson, R. Ahmad, A. DeSantolo, and Z. Várallyay, "High average power, 10 ghz pulses from a very-large-mode-area, er-doped fiber amplifier," JOSA B **34**, A1–A6 (2017).
25. A. Kumar, M. Rehan, and V. Rastogi, "Design of a large-mode-area tapered fiber amplifier for amplification of ultrashort laser pulses at 1535 nm wavelength," Optik **291**, 171377 (2023).
26. X. Chen, W. Lin, W. Wang, *et al.*, "High-power femtosecond all-fiber laser system at 1.5 μm with a fundamental repetition rate of 4.9 ghz," Opt. Lett. **46**, 1872–1875 (2021).